ORIGINAL CONTRIBUTION

Progression of Corpus Callosum Atrophy in Alzheimer Disease

Stefan J. Teipel, MD; Wolfram Bayer, MD; Gene E. Alexander, PhD; York Zebuhr, MD; Diane Teichberg; Luka Kulic, MD; Marc B. Schapiro, MD; Hans-Jürgen Möller, MD; Stanley I. Rapoport, MD; Harald Hampel, MD

Background: Atrophy of the corpus callosum in the absence of primary white matter degeneration reflects loss of intracortical projecting neocortical pyramidal neurons in Alzheimer disease (AD).

Objectives: To determine individual rates of atrophy progression of the corpus callosum in patients with AD and to correlate rates of atrophy progression with clinical disease severity and subcortical disease.

Methods: Magnetic resonance imaging–derived measurements of corpus callosum size were studied longitudinally in 21 patients clinically diagnosed as having AD (mean observation time, 17.0±8.5 months) and 10 age- and sex-matched healthy controls (mean observation time, 24.1±6.8 months).

Results: Corpus callosum size was significantly reduced in AD patients at baseline. Annual rates of atrophy of total corpus callosum, splenium, and rostrum were significantly larger in AD patients (–7.7%, –12.1%, and –7.3%, respectively) than in controls (–0.9%, –1.5%, and 0.6%, respectively). Rates of atrophy of the corpus callosum splenium were correlated with progression of dementia severity in AD patients ($\rho=0.52$, $P<.02$). The load of subcortical lesions at baseline ($P<.05$) predicted rate of anterior corpus callosum atrophy in healthy controls. Rates of atrophy of corpus callosum areas were independent of white matter hyperintensity load in patients with AD.

Conclusions: Measurement of corpus callosum size allows in vivo mapping of neocortical neurodegeneration in AD over a wide range of clinical dementia severities and may be used as a surrogate marker for evaluation of drug efficacy.

Arch Neurol. 2002;59:243-248

From the Dementia and Neuroimaging Section, Department of Psychiatry, Ludwig-Maximilian University, Munich, Germany (Drs Teipel, Bayer, Zebuhr, Kulic, Möller, and Hampel); Arizona Alzheimer's Research Center and Department of Psychology, Arizona State University, Tempe (Dr Alexander); Brain Physiology and Metabolism Section, National Institute on Aging, National Institutes of Health, Bethesda, Md (Ms Teichberg and Dr Rapoport); and Department of Pediatric Neurology, Children Hospital Medical Center, Cincinnati, Ohio (Dr Schapiro).

THE FIBERS of the corpus callosum arise predominantly from large pyramidal neurons in layers III and V of association neocortex.[1,2] These neurons form a subset of the intracortical projecting pyramidal neurons that have been shown in neuropathologic studies on postmortem brain specimens to be early and specifically affected by Alzheimer disease (AD) pathological characteristics.[3,4] Consistent with the dropout of the callosally projecting neurons, several studies[5-12] reported significant atrophy of the corpus callosum in AD. We recently described a regional pattern of corpus callosum atrophy in AD that was independent of primary white matter degeneration and was related to clinical stages of disease.[13,14] Atrophy of specific areas of the corpus callosum is correlated with the pattern of cortical metabolic decline as measured by positron emission tomography.[12,15] On this basis, we propose region-specific corpus callosum atrophy as an indirect marker for the loss of intracortical projecting neurons.

In the present study, we used structural magnetic resonance imaging (MRI) to investigate the longitudinal course of regional corpus callosum atrophy in 21 AD patients compared with 10 healthy, age- and sex-matched control subjects. We investigated whether progression of corpus callosum atrophy was related to progression of clinical disease severity in individual patients. In addition, we assessed whether the load of subcortical lesions at baseline would predict rates of atrophy progression in AD or healthy aging. To our knowledge, this is the first study to show progression of corpus callosum atrophy in AD and healthy aging.

RESULTS

CROSS-SECTIONAL ANALYSES

There was a statistically significant difference between AD patients and healthy con-

PATIENTS AND METHODS

PATIENT SELECTION

We studied at baseline 27 patients (mean±SD age, 69.2±9.3 years; 13 women and 14 men) with the clinical diagnosis of probable AD according to the National Institute of Neurological and Communicative Disorders and Stroke and the Alzheimer's Disease and Related Disorders Associations criteria.[16] For comparison, 28 healthy volunteers (68.2±8.5 years; 15 women and 13 men) were selected. Groups were matched for age and sex.

With the exception of 8 AD patients and 1 healthy control subject, all subjects had been included in previously published cross-sectional studies on corpus callosum atrophy in AD.[13-15] Cognitive impairment in the AD patients was assessed using the Mini-Mental State Examination (MMSE).[17] Mean±SD disease duration was 6.4±3.0 years in the AD patients, with an average age of onset of 62.8±8.3 years. Subgroups of 21 AD patients and 10 controls were studied longitudinally with MRI. Two patients had severe (MMSE score <10), 10 patients had moderate (MMSE score ≥10 but <20), and 9 patients had mild (MMSE ≥20) dementia. Six patients from the cross-sectional group had not been included in the longitudinal analysis. Three patients were too severely impaired to undergo MRI at follow-up; 1 of these patients died 2 years after MRI and was confirmed to have AD by autopsy. Two patients were followed up with a different MRI sequence. One patient who was moderately impaired at baseline did not return for follow-up. The cross-sectional group and the longitudinal subgroup of AD patients were not different in sex distribution or age ($P=.9$), but the MMSE score was marginally different between groups with higher values in the longitudinal subgroup ($P=.09$). Fourteen AD patients and all 10 control subjects were studied twice with MRI; 6 AD patients underwent 3 MRI scans; and 1 AD patient underwent 4 MRI scans. The AD patients were followed up between 5.1 and 31.3 months (mean±SD, 17.0±8.5 months), and the healthy controls were followed up between 11.9 and 31.7 months (24.1±6.8 months). Mean observation time was significantly shorter in the AD group compared with controls ($t_{29}=-2.3$, $P<.03$). Two MRI scans from 2 AD patients were discarded because of unsatisfactory image quality because of movement artifacts. In both cases, the scans were the first in a series of 3 MRI scans. Clinical and demographic data for the longitudinal group are presented in **Table 1**.

Significant medical comorbidity in the AD patients and controls was excluded by history, physical and neurologic examination, psychiatric evaluation, chest x-ray examination, electrocardiogram, electroencephalogram, brain MRI, and laboratory tests (complete blood cell count; erythrocyte sedimentation rate; electrolytes, glucose, blood urea nitrogen, creatinine, liver-associated enzymes, cholesterol, high-density lipoprotein, triglycerides, antinuclear antibodies, and rheumatoid factor measurement; VDRL test; human immunodeficiency virus test; serum B_{12} and folate measurement; thyroid function tests; and urine analysis). All subjects were free from clinical risk factors of cerebrovascular disease such as hypertension and diabetes. All patients were free of specific antidementive treatment. All subjects or the holders of their durable power of attorney signed consent forms to undergo MRI and neuropsychological assessment for clinical investigation and research. The protocol was approved by the National Institute of Neurological Disease and Stroke's Institutional Review Board.

MAGNETIC RESONANCE IMAGING

An axially oriented double-echo sequence (slice thickness, 6 mm; repetition time/echo time, 2000/80 and 2000/20, respectively) and a sagittally oriented T1-weighted volumetric sequence (slice thickness, 2 mm; in-plane resolution, 1×1 mm; repetition time/echo time, 20/6; flip angel, 45°) were obtained using a 0.5-T magnetic resonance tomograph (Picker Instruments, Cleveland, Ohio).

DATA PREPROCESSING

Volumetric data were manually aligned to the interhemispheric plane. To adjust the individual scans for differences in global intensity, background intensity of each scan was determined as the mean pixel intensity of a 15×15-mm^2 region of interest averaged over all slices. The region of interest always was placed in the upper left corner of the field of view. Intensity values of all scans were then scaled to have the same mean background intensity.

Preprocessing and subsequent measurements were done using ANALYZE software (Biomedical Imaging Resource, Mayo Foundation, Rochester, Minn) on an SGI workstation (Silicon Graphics, Palo Alto, Calif). All measurements were performed by one investigator (W.B.) who was masked to clinical information. Scans were analyzed

trols in total corpus callosum area ($P<.002$) at baseline, with smaller area in the AD patients. Reduction of corpus callosum area was predominant in subregions C1 (rostrum and genu) and C5 (isthmus and splenium) ($P<.02$ and $P<.001$, respectively), whereas subregions C2 to C4, representing corpus callosum truncus, remained relatively spared. Statistical significance of results remained unchanged, when areas were normalized to intracranial volume (area/intracranial volume) to correct for differences in head size. Absolute values and percentage of differences between group for corpus callosum sizes are given in **Table 2**.

In the AD group, MMSE score and age explained a significant amount of the variance of total corpus callosum area ($\beta=0.38$ and -0.41, respectively; $P<.05$). Intracranial volume, anterior and posterior WMH load, and sex did not contribute explanatory power to the model.

In the healthy control group, total cranial volume explained a significant amount of variance of total corpus callosum area ($\beta=0.72$, $P<.001$). Anterior and posterior WMH load, age, and sex did not contribute explanatory power to the model.

LONGITUDINAL ANALYSES

There was a significant difference in percent rates of change of areas over time for total corpus callosum. There was a significant effect of diagnosis on corpus cal-

in randomized order with the investigator blinded to a subject's identity.

CORPUS CALLOSUM AREA MEASUREMENTS

The areas of the corpus callosum and of 5 callosal subregions were measured in the midsagittal slice of the 3-dimensional MRI, as described elsewhere.[13] Briefly, the total callosal area was obtained by manually tracing the outer edge of the corpus callosum on the midsagittal slice. Subsequently, areas of 5 callosal subregions were defined. Subregions were labeled C1 to C5 in rostral-occipital direction, with region C1 covering the callosal rostrum and genu; regions C2, C3, and C4, the anterior, middle, and posterior truncus, respectively; and region C5, the callosal isthmus and splenium. The number of pixels within each region was summed and multiplied by pixel size to obtain absolute values (in square millimeters) for the measured areas.

The intraclass correlation coefficient for interrater reliability (determined from 10 scans measured by 2 independent researchers [S.J.T. and W.B.]) ranged from 0.98 for total corpus callosum area and subregions C1 and C2 to 0.95 for region C3. The relative error of measurement for total corpus callosum areas was 2.7%±1.3%, ranging from 3.0%±1.6% for subregion C5 and 5.7%±2.7% for subregion C3. The intraclass correlation coefficient for intrarater reliability (determined from 10 scans measured twice by the same researcher, blinded to scan identity [W.B.]) was 0.98 for total callosal area with a relative error of measurement of 1.8%±1.5%.

MEASUREMENT OF TOTAL INTRACRANIAL VOLUME

Total intracranial volume was manually traced on the 3-dimensional MRI at the inner edge of the dura. Each pixel represents a volume element (voxel) of the size 1×1 mm in the sagittal plane and 1.5 mm in the right-left axis. All voxels belonging to the traced regions of interest were summed over all slices to obtain a measure of intracranial volume.

GRADING OF WHITE MATTER HYPERINTENSITIES

The extent of white matter hyperintensities (WMH) was assessed in the axial T2-weighted MRI sequence according to a previously reported rating scale.[18] We obtained scores for WMH in the frontal, parietal, occipital, and temporal lobes. Scores for parietal, occipital, and temporal lobes were summed to obtain WMH for posterior brain, as previously described.[14] The intraclass correlation coefficient for interrater reliability (2 independent researchers rating 10 randomly selected MRI scans) was 0.65 for total WMH, 0.65 for frontal WMH, and 0.62 for posterior WMH load.

STATISTICAL ANALYSIS

The primary end point of the analyses was the annual percent change in corpus callosum areas for each individual subject. In the case of more than 2 observations, the individual annual rates of change were determined as the slope of the linear regression of time of follow-up (in months) on corpus callosum areas. In the case of only 2 observations, individual rates of atrophy were determined as the areas of corpus callosum on image 2 – image 1 divided by the duration between both images (in months). Individual rates of change were then divided by region size at baseline and multiplied by 12 months to obtain percent rates of change per year.

A group-by-subregion interaction for individual percent rates of change was assessed by repeated-measures analysis of variance with diagnosis as between-subjects factor and the percent rate of change of the 5 corpus callosum subregions as within-subject factor. A significant overall effect was followed up by pairwise single-effect analyses using the Student *t* test.

Using a stepwise linear multiple regression model, within the AD and the control groups, individual percent rates of change were predicted by age at baseline, sex, anterior and posterior WMH load, length of observation time, and, in the AD group, rate of point loss in MMSE score. In the first step, all variables were forced into the equation to assess the amount of variance explained by the selected model. Variables were then stepwise removed from the model when the amount of explained variance, which was contributed to the model, was below a threshold of $F = 2.71$ (corresponding to $P = .10$).

Differences in mean total and regional corpus callosum cross-sectional areas between AD patients and controls were assessed using the *t* test. The level of significance was determined at $P < .05$. Analyses were performed using the Statistical Package for the Social Sciences, release 9.0.1 (SPSS Inc, Chicago, Ill).

losum subregion ($P < .005$). In the single-effect analyses, percent rates of change of callosal subregions C1 (rostrum, genu), C2 (genu, anterior truncus), and C5 (isthmus, splenium) were significantly different between AD patients and controls. Mean percent rates of change for total corpus callosum were –7.7% per year in AD patients and –0.9% in healthy control subjects (**Table 3**). Because mean observation times were different between AD patients and healthy controls, we repeated the analyses with a subgroup of 16 AD patients who were matched in observation time to the healthy controls ($P = .16$). There was a significant difference between percent rates of atrophy of total corpus callosum and callosal subregions C1 and C5 between AD patients and healthy controls ($P < .05$). The difference for region C2 was not significant ($P = .83$).

The individual trajectories of atrophy progression are illustrated in **Figure 1**. In the AD group, annual point loss in MMSE score was correlated significantly with percent reduction of corpus callosum area C5, both within the full regression model ($\beta = 0.446$, $P < .03$), controlling for age, sex, observation time, and WMH load, and in the single-effect analysis ($\rho = 0.52$, $P < .02$) (**Figure 2**). No other area reduction of the corpus callosum was related to point loss in MMSE score. There was no correlation between percent rate of atrophy of total corpus callosum or any corpus callosum subregion with age, sex, time of observation, or load of frontal or posterior WMH.

Table 1. Clinical and Demographic Data at Baseline for the Longitudinal Group

Group	Age, Mean (SD) [Range], y*	F/M†	Mini-Mental State Examination Score, Mean (SD) [Range]	Total White Matter Hyperintensity Load (Range)‡
Healthy controls (n = 10)	65.4 (7.2) [52-76]	4/6	29.8 (0.4) [29-30]	1.5 (0.0-4.0)
Patients with Alzheimer disease (n = 21)	69.2 (8.2) [54-87]	10/11	17.4 (6.7) [1-28]	2.0 (0.0-6.3)

*Not different between groups, $t_{29} = 1.27$, $P = .22$.
†Not different between groups, $\chi^2_1 = 0.16$, $P = .69$.
‡Data in parentheses indicate the median (25th and 75th percentile) and maximal possible range on a scale of 0 to 24, not different between groups, Mann-Whitney U test = 95.5, $P = .68$.

Table 2. Cross-sectional Atrophy of Corpus Callosum*

Region	Healthy Controls (n = 28)	AD Patients (n = 27)	% Difference for AD vs Controls†	% Difference for AD vs Controls‡
TCA	506.1 ± 93.2	427.5 ± 87.6	−16§	−15§
C1	137.2 ± 34.6	114.5 ± 30.5	−17‖	−16‖
C2	65.4 ± 16.1	59.6 ± 17.5	−9	−6
C3	63.5 ± 13.0	59.3 ± 12.0	−7	−6
C4	61.9 ± 14.6	57.1 ± 17.5	−8	−6
C5	153.2 ± 27.6	116.4 ± 27.7	−24¶	−23¶

*Data are presented as mean ± SD areas of total corpus callosum (TCA) and 5 subregions (C1 to C5) in square millimeters. AD indicates Alzheimer disease.
†For absolute values.
‡For values normalized to intracranial volume.
§Significant difference between patients with AD and controls ($P<.002$).
‖Significant difference between patients with AD and controls ($P<.02$).
¶Significant difference between patients with AD and controls ($P<.001$).

Table 3. Atrophy Progression of Corpus Callosum*

Region	Healthy Controls (n = 10)	AD Patients (n = 21)
TCA	−0.9 ± 5.0	−7.7 ± 6.7†
C1	−1.6 ± 6.3	−12.1 ± 15.1‡
C2	3.9 ± 12.1	−10.3 ± 18.8‡
C3	−1.6 ± 9.5	−3.0 ± 10.6
C4	−3.7 ± 12.7	4.0 ± 18.1
C5	0.7 ± 3.6	−7.3 ± 9.3‡

*Data are presented as mean ± SD percent rates of atrophy for total corpus callosum (TCA) and 5 corpus callosum subregions (C1 to C5). AD indicates Alzheimer disease.
†Significantly different between patients with AD and healthy controls at $P<.01$.
‡Significantly different between patients with AD and healthy controls at $P<.05$.

In the control group, percent rate of atrophy of anterior corpus callosum area C2 was correlated significantly with anterior WMH load ($\beta = -0.90$, $P<.05$) and sex ($\beta = 0.85$, $P<.05$), with greater rates of area reduction in women. There was no correlation with posterior WMH load, age, or time of observation. There also was no correlation between percent rate of atrophy of other corpus callosum areas and WMH load at baseline.

COMMENT

In the present study, we investigated the longitudinal progression of corpus callosum atrophy in AD and healthy aging. Based on previous evidence from cross-sectional studies, we expected greater atrophy progression in AD patients than in healthy subjects. We further expected that in AD patients who were free of clinical risk factors for cerebrovascular disease, atrophy progression of corpus callosum would be independent of the extent of subcortical lesions.

We found an overall reduction of corpus callosum area by roughly 7.7% per year in AD patients compared with 0.9% per year in healthy controls. The rate of atrophy was significantly greater in AD patients compared with controls in rostrum and splenium of the corpus callosum, regions that were the most severely affected during cross-sectional comparisons. The truncus remained relatively preserved in the cross-sectional and the longitudinal analyses.

In the healthy control subjects, the extent of frontal lobe WMH predicted the rate of area reduction of the anterior corpus callosum. Because WMH are commonly regarded as measures of primary subcortical disease,[19] this association suggests that age-related atrophy of the anterior corpus callosum in healthy subjects results from primary subcortical lesions to fiber tracts crossing the frontal lobe white matter. This finding agrees with neuropathologic evidence for predominant frontal lobe involvement of cerebral white matter in cerebrovascular disease.[20] This further agrees with a significant correlation between frontal lobe WMH load and anterior corpus callosum atrophy in healthy, elderly subjects in a cross-sectional study.[14] This interpretation, however, needs further confirmation in an independent sample because the group of healthy subjects was small in our study and the range of subcortical lesions was low.

In contrast, in the AD patients, longitudinal progression of regional corpus callosum atrophy mainly re-

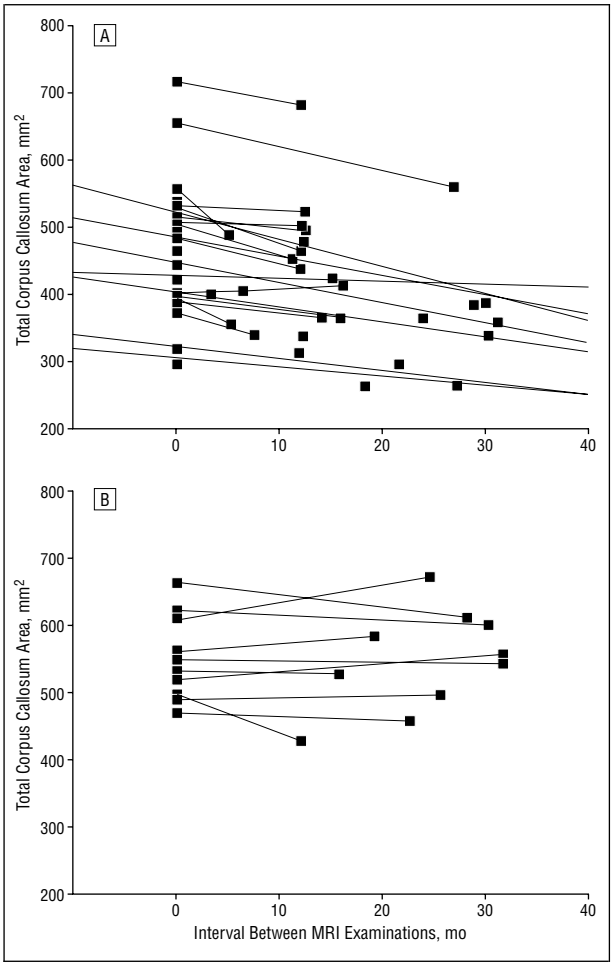

Figure 1. Trajectories of corpus callosum atrophy in 21 patients with Alzheimer disease (A) and 10 healthy, elderly control subjects (B). MRI indicates magnetic resonance imaging.

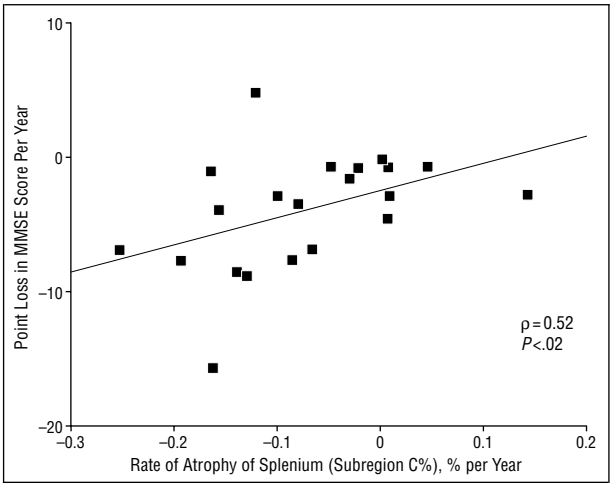

Figure 2. Correlation between the atrophy rate of corpus callosum subregion C5 and Mini-Mental State Examination (MMSE) score difference in 21 patients with Alzheimer disease.

sults from loss of callosally projecting cortical neurons. Neuron loss as the main cause of atrophy then would mask any additional effect from primary lesions to the callosally projecting fibers in subcortical white matter. This notion is first supported by the lack of difference in the extent of WMH between AD patients and healthy controls. In addition, rate of atrophy progression in AD patients was independent from the extent of WMH. It also agrees with previous findings of statistically significant correlations between regional cortical hypometabolism as a measure of cortical neuronal integrity and regional corpus callosum atrophy independent of WMH load in AD patients.[12,15]

It has been estimated from postmortem studies that about 30% of intracortical association neurons are lost in layers III and V of neocortex in AD patients.[21] Corpus callosum fibers arise from a subset of these neurons.[1,2] Neocortical neuron loss, as shown in neuropathologic studies and reflected by cortical metabolic decline, is most pronounced in the temporal and parietal association areas[21,22] that send interhemispheric projections through corpus callosum isthmus and splenium (corresponding to region C5).[23-25] Less neuron loss is seen in frontal association cortex projecting through the rostrum (corresponding to region C1). Primary sensory motor areas that project through the corpus callosum truncus are least affected.

The significant correlation between progression of splenium atrophy and the progression of clinical disease severity as measured by the MMSE in the AD patients is in agreement with the outlined fiber topography, since loss of functional integrity in the parietal and temporal association areas that project through corpus callosum splenium is closely related to disease severity.[26] Decline in MMSE score explained about 27% of variance between individual trajectories of atrophy in splenium in the AD patients. This suggests that a considerable part of the variance in our longitudinal measures reflects clinically meaningful differences in the course of the disease. It is likely that variability in repeated measurements contributed to the high variability in longitudinal measures of corpus callosum subregions. It may also in part account for the positive rates of change found in area C3 in AD patients and in area C2 in controls. In addition, the variability in observation time may contribute to variability in rates of change because shorter length of observation time may lead to less accurate assessment of the rate of change, particularly when rates of change are not linear over all stages of disease.

In summary, we investigated the longitudinal rate of corpus callosum atrophy in AD patients compared with healthy age-matched controls. Rates of atrophy progression were significantly greater in AD patients compared with controls. Progression of clinical disease severity was correlated with progression of atrophy of the corpus callosum. Atrophy of the corpus callosum, independently of primary white matter degeneration, reflects loss of intracortical projecting pyramidal neurons in the neocortex. Therefore, we propose longitudinal corpus callosum measurement as a surrogate marker of progressive neocortical neuronal degeneration in AD[27] if the results of this first longitudinal study can be confirmed in an independent sample. Measurement of corpus callosum areas in vivo may help to map efficacy of pharmacologic intervention on the progression of morphologic changes in AD patients free of cerebrovascular disease.

Accepted for publication September 12, 2001.

Author contributions: *Study concept and design* (Drs Teipel, Alexander, Schapiro, Rapoport, and Hampel); *acquisition of data* (Drs Teipel, Bayer, Alexander, Zebuhr, and Kulic and Ms Teichberg); *analysis and interpretation of data* (Drs Teipel, Alexander, Möller, Rapoport, and Hampel); *drafting of the manuscript* (Drs Teipel, Bayer, and Hampel and Ms Teichberg); *critical revision of the manuscript for important intellectual content* (Drs Bayer, Alexander, Zebuhr, Kulic, Schapiro, Möller, Rapoport, and Hampel and Ms Teichberg); *statistical expertise* (Drs Teipel, Alexander, Möller, and Hampel); *obtained funding* (Drs Teipel and Hampel); *administrative, technical, and material support* (Drs Bayer, Zebuhr, Rapoport, Kulic, and Schapiro and Ms Teichberg); *study supervision* (Drs Möller, Rapoport, and Hampel).

This study was supported in part by a grant from Eisai (Frankfurt) and Pfizer (Karlsruhe) (Drs Hampel and Teipel), and by a grant from the Medical Faculty of the Ludwig-Maximilian University, Munich (Dr Teipel), Germany.

Portions of this article originate from the doctoral thesis of Dr Bayer (Ludwig-Maximilian University, Munich, Germany; in preparation).

We thank A. W. L. Bokde, PhD, Department of Psychiatry, Ludwig-Maximilian University, for helpful discussion.

Corresponding author and reprints: Stefan J. Teipel, MD, and Harald Hampel, MD, Dementia and Neuroimaging Section, Department of Psychiatry, Ludwig-Maximilian University, Nussbaumstr 7, 80336 Munich, Germany (e-mail: stt@psy.med.uni-muenchen.de).

REFERENCES

1. Conti F, Manzoni T. The neurotransmitters and postsynaptic actions of callosally projecting neurons. *Behav Brain Res.* 1994;64:37-53.
2. Innocenti GM, Aggoun-Zouaoui D, Lehmann P. Cellular aspects of callosal connections and their development. *Neuropsychologia.* 1995;33:961-987.
3. Mann DM. Pyramidal nerve cell loss in Alzheimer's disease. *Neurodegeneration.* 1996;5:423-427.
4. Armstrong RA. Is the clustering of neurofibrillary tangles in Alzheimer's patients related to the cells of origin of specific cortico-cortical projections? *Neurosci Lett.* 1993;160:57-60.
5. Biegon A, Eberling JL, Richardson BC, et al. Human corpus callosum in aging and Alzheimer's disease: a magnetic resonance imaging study. *Neurobiol Aging.* 1994;15:393-397.
6. Cuénod C-A, Denys A, Michot J-L, et al. Amygdala atrophy in Alzheimer's disease: an in vivo magnetic resonance imaging study. *Arch Neurol.* 1993;50:941-945.
7. Janowsky JS, Kaye JA, Carper RA. Atrophy of the corpus callosum in Alzheimer's disease versus healthy aging. *J Am Geriatr Soc.* 1996;44:798-803.
8. Lyoo K, Satlin A, Lee CK, Renshaw PF. Regional atrophy of the corpus callosum in subjects with Alzheimer's disease and multi-infarct dementia. *Psychiatry Res.* 1997;74:63-72.
9. Pantel J, Schröder J, Essig M, et al. Corpus callosum in Alzheimer's disease and vascular dementia: a quantitative magnetic resonance study. *J Neural Transm.* 1998;54(suppl):129-136.
10. Vermersch P, Roche J, Hamon M, et al. White matter magnetic resonance imaging hyperintensity in Alzheimer's disease: correlations with corpus callosum atrophy. *J Neurol.* 1996;243:231-234.
11. Weis S, Jellinger K, Wenger E. Morphometry of the corpus callosum in normal aging and Alzheimer's disease. *J Neural Transm.* 1991;33(suppl):35-38.
12. Yamauchi H, Fukuyama H, Harada K, et al. Callosal atrophy parallels decreased cortical oxygen metabolism and neuropsychological impairment in Alzheimer's disease. *Arch Neurol.* 1993;50:1070-1074.
13. Hampel H, Teipel SJ, Alexander GE, et al. Corpus callosum atrophy is a possible indicator for region and cell type specific neuronal degeneration in Alzheimer disease: an MRI analysis. *Arch Neurol.* 1998;55:193-198.
14. Teipel SJ, Hampel H, Alexander GE, et al. Dissociation between white matter pathology and corpus callosum atrophy in Alzheimer's disease. *Neurology.* 1998; 51:1381-1385.
15. Teipel SJ, Hampel H, Pietrini P, et al. Region specific corpus callosum atrophy correlates with regional pattern of cortical glucose metabolism in Alzheimer's disease. *Arch Neurol.* 1999;56:467-473.
16. McKhann G, Drachman D, Folstein M, Katzman R, Price D, Stadlan EM. Clinical diagnosis of Alzheimer's disease: report of the NINCDS-ADRDA Work Group under the auspices of the Department of Health and Human Services Task Force on Alzheimer's Disease. *Neurology.* 1984;34:939-944.
17. Folstein MF, Folstein SE, McHugh PR. Mini-mental state: a practical method for grading the cognitive state of patients for the clinician. *J Psychiatr Res.* 1975; 12:189-198.
18. Scheltens P, Barkhof F, Leys D, et al. A semiquantitative rating scale for the assessment of signal hyperintensities on magnetic resonance imaging. *J Neurol Sci.* 1993;114:7-12.
19. Awad IA, Johnson PC, Spetzler RF, Hodak JA. Incidental subcortical lesions identified on magnetic resonance imaging in the elderly, II: postmortem pathological correlations. *Stroke.* 1986;17:1090-1097.
20. Yamanouchi H, Sugiura S, Tomonaga M. Decrease in nerve fibres in cerebral white matter in progressive subcortical vascular encephalopathy of Binswanger type. *J Neurol.* 1989;236:382-387.
21. Terry R, Katzman R. Senile dementia of the Alzheimer type: defining a disease. In: Terry R, Katzman R, eds. *The Neurology of Aging.* Philadelphia, Pa: FA Davis Co; 1983:51-84.
22. Kumar A, Schapiro MB, Grady C, et al. High resolution PET studies in Alzheimer's disease. *Neuropsychopharmacology.* 1991;4:35-46.
23. Pandya DN, Seltzer B. The topography of commissural fibres. In: Lepre F, Ptito M, Jasper HH, eds. *Two Hemispheres–One Brain: Functions of the Corpus Callosum.* New York, NY: Alan R Liss Inc; 1986:47-73.
24. De Lacoste MC, Kirkpatrick JB, Ross ED. Topography of the human corpus callosum. *J Neuropathol Exp Neurol.* 1985;44:578-591.
25. Tan YL, Chen BH, Yang JD, et al. Localization of functional projections from corpus callosum to cerebral cortex. *Chin Med J.* 1991;104:851-857.
26. Heiss WD, Herholz K, Pawlik G, Wagner R, Wienhard K. Positron emission tomography in neuropsychology. *Neuropsychologia.* 1986;24:141-149.
27. Hampel H, Teipel SJ, Alexander GE, et al. Corpus callosum measurement is an in vivo indicator for neocortical neuronal integrity, but not white matter pathology, in Alzheimer's disease. *Ann N Y Acad Sci.* 2000;903:470-477.